Glutathionylation and Reduction of Methacrolein in Tomato Plants Account for Its Absorption from the Vapor Phase[1][OPEN]

Shoko Muramoto, Yayoi Matsubara, Cynthia Mugo Mwenda, Takao Koeduka, Takuya Sakami, Akira Tani, and Kenji Matsui*

Department of Biological Chemistry, Faculty of Agriculture, and Department of Applied Molecular Bioscience, Graduate School of Medicine, Yamaguchi University, Yamaguchi 753–8515, Japan (S.M., Y.M. C.M.M., T.K., K.M.); and Institute for Environmental Sciences, University of Shizuoka, Shizuoka 422–8526, Japan (T.S., A.T.)

ORCID IDs: 0000-0002-2797-3908 (C.M.M.); 0000-0002-4875-5176 (K.M.).

A large portion of the volatile organic compounds emitted by plants are oxygenated to yield reactive carbonyl species, which have a big impact on atmospheric chemistry. Deposition to vegetation driven by the absorption of reactive carbonyl species into plants plays a major role in cleansing the atmosphere, but the mechanisms supporting this absorption have been little examined. Here, we performed model experiments using methacrolein (MACR), one of the major reactive carbonyl species formed from isoprene, and tomato (*Solanum lycopersicum*) plants. Tomato shoots enclosed in a jar with MACR vapor efficiently absorbed MACR. The absorption efficiency was much higher than expected from the gas/liquid partition coefficient of MACR, indicating that MACR was likely metabolized in leaf tissues. Isobutyraldehyde, isobutyl alcohol, and methallyl alcohol (MAA) were detected in the headspace and inside tomato tissues treated with MACR vapor, suggesting that MACR was enzymatically reduced. Glutathione (GSH) conjugates of MACR (MACR-GSH) and MAA (MAA-GSH) were also detected. MACR-GSH was essentially formed through spontaneous conjugation between endogenous GSH and exogenous MACR, and reduction of MACR-GSH to MAA-GSH was likely catalyzed by an NADPH-dependent enzyme in tomato leaves. Glutathionylation was the metabolic pathway most responsible for the absorption of MACR, but when the amount of MACR exceeded the available GSH, MACR that accumulated reduced photosynthetic capacity. In an experiment simulating the natural environment using gas flow, MACR-GSH and MAA-GSH accumulation accounted for 30% to 40% of the MACR supplied. These results suggest that MACR metabolism, especially spontaneous glutathionylation, is an essential factor supporting MACR absorption from the atmosphere by tomato plants.

Plants emit vast amounts of volatile organic chemicals (VOCs) into the atmosphere. The annual emission of VOCs other than methane is estimated to be approximately 1,300 Tg of carbon (Goldstein and Galbally, 2007), with approximately 90% originating from biogenic sources, of which one-third (approximately 500 Tg of carbon/year) is isoprene (Guenther et al., 1995). In the atmosphere, VOCs undergo the chemical processes of photolysis and reaction with hydroxyl and nitrate radicals (Atkinson and Arey, 2003). Isoprene, for example, is converted into a series of isomeric hydroxyl-substituted alkyl peroxyl radicals, which are further converted into methyl vinyl ketone (MVK; but-3-en-2-one) and methacrolein (MACR; 2-methylprop-2-enal; Liu et al., 2013). These VOCs and their oxygenated products (oVOCs) are important components for the production of ozone and aerosols, and thus have a big impact on atmospheric chemistry and even on the climate system (Goldstein and Galbally, 2007). VOCs and oVOCs are removed from the atmosphere through oxidation to carbon monoxide or dioxide, dry or wet deposition, or secondary aerosol formation (Goldstein and Galbally, 2007). Among these, deposition to vegetation plays a major role in the removal of VOCs and oVOCs from the atmosphere (Karl et al., 2010).

A significant portion of the deposition to vegetation is attributable to the uptake of VOCs and oVOCs by plants, and a field study showed that MVK and MACR were immediately lost once they entered a leaf through stomata (Karl et al., 2010). Under growth conditions where stomatal conductance is high enough, the partitioning of VOCs between air and leaf water phases in equilibrium and the capacity of the plant to metabolize, translocate, and store VOCs determine their uptake rate (Tani et al., 2013). The immediate loss in leaves

[1] This work was supported by the Japan Society for the Promotion of Sciences KAKENHI (grant nos. 26660095 and 25282234) and the Yobimizu Project from Yamaguchi University.

* Address correspondence to matsui@yamaguchi-u.ac.jp

The author responsible for distribution of materials integral to the findings presented in this article in accordance with the policy described in the Instructions for Authors (www.plantphysiol.org) is: Kenji Matsui (matsui@yamaguchi-u.ac.jp).

S.M. performed most of the experiments; Y.M., C.M.M., T.K., and T.S. provided technical assistance to S.M.; A.T. supervised parts of the project and edited the article; K.M. designed and supervised the experiments, analyzed the data, and wrote the article.

[OPEN] Articles can be viewed without a subscription.

www.plantphysiol.org/cgi/doi/10.1104/pp.15.01045

observed with MVK and MACR is indicative of efficient enzymatic reactions metabolizing them; however, the details of the metabolism of these oVOCs have been little investigated so far.

The absorption and metabolism of several VOCs by plants have been reported. Airborne *ent*-kaurene was absorbed by Arabidopsis (*Arabidopsis thaliana*), Japanese cypress (*Chamaecyparis obtusa*), and Japanese cedar (*Cryptomeria japonica*) plants and converted into GAs (Otsuka et al., 2004). Arabidopsis absorbed (*Z*)-3-hexenal and converted it into (*Z*)-3-hexen-1-ol or further into (*Z*)-3-hexen-1-yl acetate using NADPH and acetyl-CoA, probably inside the plant tissues (Matsui et al., 2012). *Nicotiana attenuata* plants absorbed dimethyl disulfide formed by rhizobacteria (Meldau et al., 2013). The sulfur atom derived from volatile dimethyl disulfide was assimilated into plant proteins. Karl et al. (2010) assumed that aldehyde dehydrogenase, which is involved in detoxification that limits aldehyde accumulation and oxidative stress (Kirch et al., 2004), is involved in the uptake of oVOCs containing an aldehyde moiety; however, they did not provide direct evidence supporting their assumption.

Conjugation of VOCs and oVOCs with sugar or glutathione (GSH) is another way to metabolize them. (*Z*)-3-Hexen-1-ol in the vapor phase was taken up by tomato (*Solanum lycopersicum*) plants and converted into its glycoside (Sugimoto et al., 2014). (*E*)-2-Hexenal reacts with GSH spontaneously and/or via glutathione *S*-transferase (GST) to form hexanal-GSH, which is subsequently reduced to hexanol-GSH (Davoine et al., 2006), although it is uncertain whether airborne (*E*)-2-hexenal is converted into its corresponding GSH adduct. Glutathionylation of (*E*)-2-hexenal is common and has been confirmed in grapevine (*Vitis vinifera*) and passion fruit (*Passiflora edulis*; Kobayashi et al., 2011; Fedrizzi et al., 2012). The catabolites formed from the GSH adduct in these crops are precursors for important flavor components.

Although it is clear that oVOCs are absorbed by vegetation and that their efficient uptake is probably supported by metabolism in plant tissues, the metabolic fates of oVOCs taken up from the vapor phase into plants have been little studied. Here, we performed a series of model experiments using tomato seedlings and MACR to dissect the fates of oVOCs once they entered into plant tissues. To clearly see absorption of MACR and its fates in plant tissues, a model experiment under enclosed conditions with a high concentration of MACR was first carried out. Subsequently, an airflow system with a realistically low concentration of MACR was used. Tomato plants efficiently absorbed MACR. Reduction of the carbonyl moiety and the double bond conjugated to the carbonyl and conjugation with GSH were the major methods of metabolism of exogenous MACR. The metabolism seemed to be involved in the detoxification of reactive carbonyl species, which, in turn, accounted for the oVOC deposition to vegetation.

RESULTS

Absorption of MACR in the Headspace by Tomato

To examine the absorption of MACR by tomato plants, we placed the aboveground parts of 3- to 4-week-old tomato plants in a glass jar (187 mL), and a droplet (9.35 μL) of MACR solution (0.5 M dissolved in 3.5% [w/v] Tween 20) was absorbed into the tip of a cotton swab. The jar was tightly closed and placed under light at 25°C. Because the partial pressure of MACR in the jar (0.427 mm Hg) that would be expected if all of the MACR was vaporized was lower than the vapor pressure of MACR (155 mm Hg) at 25°C, the MACR concentration would be 560 μL L^{-1}. A jar without a plant was used as a control. The headspace gas was sampled periodically, and the airborne carbonyl compounds in the headspace were quantified with HPLC after derivatization into their 2,4-dinitrophenylhydrazones. When the headspace was taken immediately (approximately 10 s) after the lid was closed, MACR was detected at its vapor concentration of 250 to 270 μL L^{-1} (Fig. 1A). Without a plant, the concentration in the headspace was 390 μL L^{-1} and remained mostly constant until 4 h. In the presence of a plant, the headspace concentration of MACR dropped to 80 μL L^{-1} by 0.5 h. The concentration continued to decrease until 4 h. At 2 h, approximately 90% of the MACR was taken up by the tomato plant.

Reduction

In HPLC analysis of the headspace gas, we noticed the appearance of a peak corresponding to isobutyraldehyde (2-methylpropanal) that would be formed through reduction of the alkene moiety of MACR. At 0 h (10 s after the onset of the experiment), isobutyraldehyde was below the detection limit, but at 0.5 h, it increased to 30 μL L^{-1} (Fig. 1B). The amount of isobutyraldehyde detected at 0.5 h corresponded to 5.8% of the MACR used for the exposure. Its concentration in the headspace then decreased, and after 2 h, it was almost undetectable. In the absence of the plant, no isobutyraldehyde formation was detected.

Previously, we showed that Arabidopsis plants absorbed (*Z*)-3-hexenal, reduced it into (*Z*)-3-hexen-1-ol, and thereafter, emitted (*Z*)-3-hexen-1-ol into the atmosphere (Matsui et al., 2012). Thus, we assumed that the reduction of aldehydes to alcohols would be one way of metabolizing airborne carbonyl compounds. To examine the reduction of the aldehyde moiety of MACR and reemission of its reduced forms by tomato plants, the aerial part of tomato plant was exposed to 560 μL L^{-1} MACR vapor in a 187-mL glass jar for 2 and 24 h, and VOCs in the headspace gas were extracted with dichloromethane and subjected to gas chromatography (GC)-mass spectrometry (MS) analysis. Under the GC-MS conditions used here, MACR and isobutyraldehyde could not be detected. No compound related to MACR was detected immediately after exposing tomato

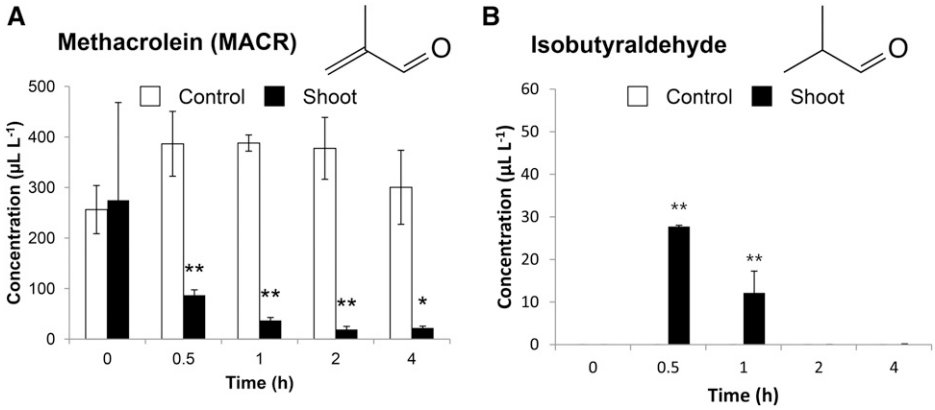

Figure 1. Absorption and reduction of MACR by tomato plants. MACR was vaporized at 560 μL L^{-1} in a glass jar (187 mL) with and without the aerial part of tomato plant (shown in black and white bars, respectively). After different incubation periods, the concentrations of MACR (A) and isobutyraldehyde (B) in the headspace were examined with HPLC after derivatization to their 2,4-dinitrophenylhydrazones. Bars represent the mean ± SE; $n = 4$. An asterisk in the figure indicates a significant difference from the control (two-way ANOVA followed by Tukey; *, $P < 0.05$; **, $P < 0.01$).

plants to MACR vapor (Fig. 2A). At 2 h after exposure, 2-methylprop-2-en-1-ol (MAA) and 2-methylpropan-1-ol (isobutyl alcohol) were detected only when MACR vapor was incubated with tomato plants (Figs. 2A; Supplemental Fig. S1). At 2 h, 0.96% and 1.6% of the MACR used for exposure was found as MAA and isobutyl alcohol in the headspace, respectively. At 24 h, their concentrations in the headspace decreased to less than 2 μL L^{-1}.

Because the reduction of carbonyls needs a reductant, such as NADH or NADPH, which are generally found inside cells, the reduction of MACR to MAA and isobutyl alcohol should proceed in the cells. Thus, we assumed that MAA and isobutyl alcohol were formed inside the tomato cells, and that a portion of each was emitted from the tissues to the headspace. Therefore, we next extracted MACR metabolites from the leaves exposed to MACR vapor at 560 μL L^{-1} in a glass jar (187 mL) for 2 and 24 h. After extraction with dichloromethane, MAA formation in plant tissues was detected even after 3 to 4 s of MACR exposure (Fig. 2B). At that time, isobutyl alcohol was not detected in the plant tissues. Both MAA and isobutyl alcohol in the tissues increased at 2 h after exposure, and then decreased to low levels at 24 h. At 2 h, 6.5% and 5.6% of the MACR used for the exposure was detected as MAA and isobutyl alcohol in the tissues, respectively. Although we did not distinguish whether these alcohols really occurred in the plant tissue or were just attached to the plant surface, these alcohols should be formed from MACR taken up from the headspace into the tissues where a reductase-catalyzed reduction was operative (Matsui et al., 2012).

Glutathionylation

It has been reported that reactive carbonyl species harboring α,β-unsaturated carbonyl moieties are detoxified through conjugation with GSH (Davoine et al.,

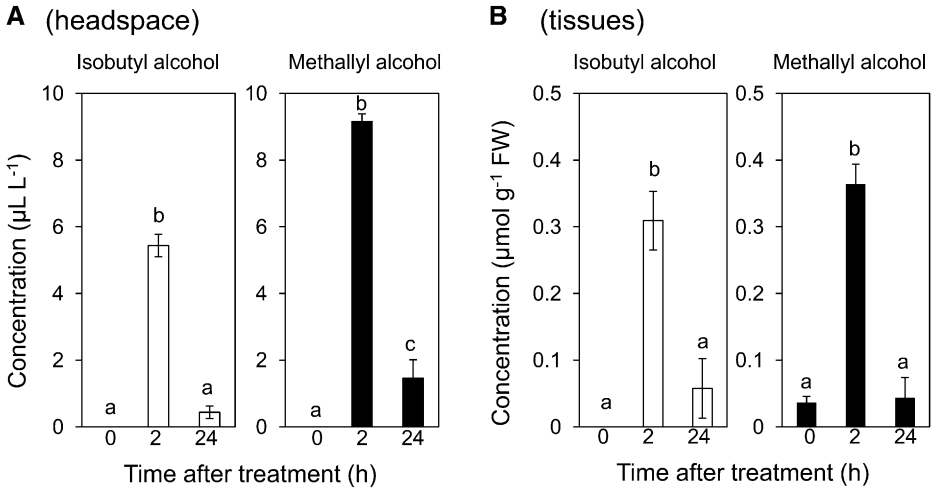

Figure 2. The amounts of reduced metabolites derived from MACR in the headspace (A) and in plant tissues (B). The aerial part of tomato plants were exposed to MACR at 560 μL L^{-1} in a closed jar (187 mL), and the amounts of isobutyl alcohol and methallyl alcohol (MAA) in the headspace and in the plant tissues were determined. These reduced metabolites were undetectable when MACR was vaporized without a plant or a plant was enclosed in the absence of MACR. Bars represent the mean ± SE; $n = 6$ (A) or 3 (B). Different letters indicate a significant difference among periods (two-way ANOVA followed by Tukey; $P < 0.05$).

2005, 2006; Mano, 2012). The conjugation reaction proceeds either spontaneously or enzymatically via GST (Davoine et al., 2006). Because MACR has the α,β-unsaturated carbonyl moiety, we assumed that a portion of the MACR taken up by tomato plants would be converted to its GSH adduct (*S*-3-[2-methylpropanal]glutathione, MACR-GSH) in the tissues. To examine the formation of the conjugate, we first synthesized MACR-GSH and established an analytical system with liquid chromatography (LC)-tandem mass spectrometry (MS/MS; Supplemental Figs. S2 and S3).

When an extract prepared from tomato plants exposed to MACR vapor at 560 μL L^{-1} in a glass jar (187 mL) for 2 h was subjected to LC-MS/MS analysis, we detected a peak corresponding to MACR-GSH. At the same time, a big peak with a mass-to-charge ratio (*m/z*) of 380 was detected. This peak coincided with the compound prepared from synthetic MACR-GSH through reduction with $NaBH_4$; thus, it was assigned as the GSH adduct of MAA (*S*-3-[2-methylpropan-1-ol]glutathione [MAA-GSH]). The MS profiles of synthetic MAA-GSH and the compound detected in the MACR-exposed tomato tissues supported this assignment (Supplemental Fig. S3). When the extract was analyzed in the neutral loss mode (−75 D; corresponding to the removal of Gly) with the aim of detecting all GSH adducts, only peaks corresponding to MACR-GSH and MAA-GSH were detected (Supplemental Fig. S4).

Next, we followed formation of MACR-GSH and MAA-GSH in tomato leaves exposed to 560 μL L^{-1} of MACR vapor in a glass jar (187 mL; Fig. 3). MACR-GSH and MAA-GSH were detected in tomato tissues even at 3 to 4 s after the onset of exposure. MACR-GSH was quickly formed, and at 1 min after exposure, the amount went up to 568 nmol g^{-1} fresh weight (FW; corresponding to 6.12% of the added MACR). The amount reached its maximum at 10 min and gradually decreased thereafter. MAA-GSH, the reduced form of MACR-GSH, started to increase from 1 min after exposure, and reached its maximum level (1,504 nmol g^{-1} FW, corresponding to 20.9% of the added MACR) at 30 min. The level was almost constant until 24 h.

GST Activity to Form MACR-GSH and Reductase Activity to Form MAA-GSH

To examine whether the formation of GSH adducts with MACR was catalyzed by GST or occurred spontaneously, we prepared a crude enzyme extract from tomato leaves and estimated the GST activity. When a common GST substrate, 1-chloro-2,4-dinitrobenzene, was used, no GST activity was detected. Spontaneous formation of MACR-GSH was detected just by mixing MACR and GSH in phosphate buffer at pH 6.5. The addition of crude enzyme solution into the reaction mixture hardly enhanced the reaction between MACR and GSH (Supplemental Fig. S5). Thus, we failed to detect, at least in vitro, significant GST activity in the formation of MACR-GSH in tomato leaves.

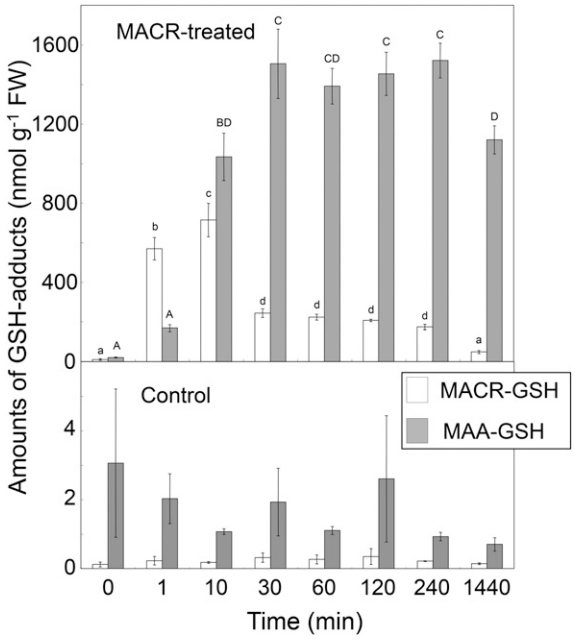

Figure 3. The amount of MACR-GSH (white bars) and MAA-GSH (gray bars) in tomato treated with MACR vapor. The aerial part of tomato was exposed to 0 (control: bottom) or 560 μL L^{-1} (MACR treated: top) MACR for 0 to 1,440 min in a glass jar (187 mL). Bars represent the mean ± SE; $n = 3$. Different letters indicate a significant difference among periods with each compound (two-way ANOVA followed by Tukey; $P < 0.05$).

MAA-GSH should be formed from MACR-GSH through reduction of the carbonyl group originating from MACR. Reduction of the aldehyde group in the GSH adduct derived from (*Z*)-3-hexenal was supposed in tobacco leaves (*Nicotiana tabacum*) and grapevine based on the metabolites found in these plant tissues (Davoine et al., 2006; Kobayashi et al., 2011). When MACR-GSH was incubated with crude enzyme solution in the presence of NADPH, MAA-GSH formation was detected (Fig. 4). The addition of NADH also enhanced MACR-GSH reduction, but to a lesser extent than NADPH. Heat-denatured enzyme solution failed to enhance the reduction even in the presence of NADPH. The MACR-GSH to MAA-GSH reduction activity was inducible, and higher activity was detected in tomato leaves exposed to MACR vapor at 560 μL L^{-1} in a glass jar (187 mL) for 2 h (Fig. 4).

MACR Absorption in a Flow System

The experimental system used in this study to expose tomato plants to MACR vapor in an enclosed jar helped us clarify the metabolism of MACR as shown above; however, in a natural environment, plants are exposed to VOCs in airflow. The concentration of MACR in natural environments ranges from 0.2 to 13.6 nL L^{-1} levels (Jardine et al., 2012, 2013; Kalogridis et al., 2014). To confirm whether the MACR metabolism in tomato plants observed in the enclosed experimental system

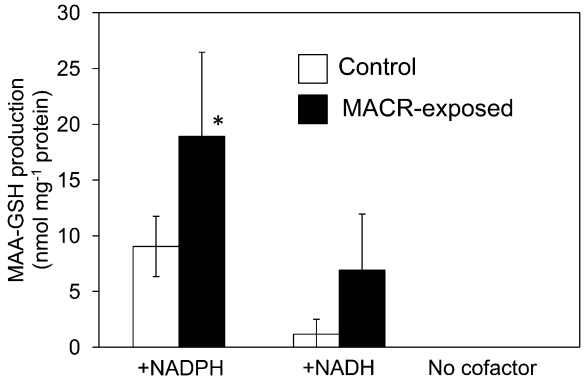

Figure 4. MACR-GSH to MAA-GSH reduction activity in the presence of NADPH, NADH, or in the absence of any cofactor in tomato shoots treated with MACR vapor (at 560 μL L^{-1} for 2 h) or air in a 187-mL glass jar. A crude enzyme extract prepared from exposed tomato leaves was reacted with MACR-GSH for 10 min; thereafter, the amount of MAA-GSH was determined by LC-MS/MS. Bars represent the mean ± SE; n = 3. An asterisk in the figure indicates a significant difference from the control (two-way ANOVA followed by Tukey; *, $P < 0.05$).

also operated in an airflow system with a realistically low concentration of MACR, we set up an airflow system to expose tomato plants (Tani et al., 2013). Because glutathionylation was the main metabolism method of MACR according to the results with the enclosed exposure system, and the sensitivity of GSH adduct detection in the LC-MS/MS system used in this study was high, we focused on glutathionylation. In our airflow system, tomato plants grown in pots were exposed to airflow containing 0, 20, or 100 nL L^{-1} MACR at 1.5 L min^{-1} in a transparent, fluorinated ethylene-propylene copolymer bag (20–40 L) for 6 h under illumination. We also set the MACR concentration at 100 nL L^{-1} to estimate the capacity of tomato plants to absorb and metabolize MACR. After exposure, leaves were harvested for LC-MS/MS analysis of the GSH adducts.

During exposure to the flow of clean air, tomato plants emitted isoprene and MACR at rates of 8.90 ± 3.58 and 4.67 ± 1.08 fmol g^{-1} FW s^{-1}, respectively. The net photosynthetic rate was largely constant at 21.2 ± 1.50 nmol (CO_2) s^{-1} plant^{-1}, and the transpiration rate was 2.44 ± 0.06 μmol (H_2O) s^{-1} plant^{-1}. Tomato plants exposed to clean air for 6 h had trace amounts of MACR-GSH and MAA-GSH (Tables I and II). After exposure to 20 nL L^{-1} MACR, accumulation of 1.47 ± 0.14 nmol g^{-1} FW MACR-GSH and 37.9 ± 2.84 nmol g^{-1} FW MAA-GSH was detected. With 100 nL L^{-1} MACR, the amounts of MACR-GSH and MAA-GSH went up to 6.51 ± 0.87 and 153 ± 15.7 nmol g^{-1} FW. Even after exposure to 100 nL L^{-1} MACR for 6 h, no visible symptoms of MACR toxicity were detected. Because we exposed five tomato plants of approximately 1 g FW in each bag, the total amounts of GSH adducts in the tomatoes in the bag were estimated to be 197 and 798 nmol, respectively, at 20 and 100 nL L^{-1} MACR. This suggested that as much as approximately 41% and 33% of the airborne MACR supplied in airflow (0.48 and 2.41 μmol, respectively) was absorbed by the tomato plants and converted into GSH adducts.

The Capacity of MACR Metabolism Is Limited

To estimate the capacity of tomato plants to absorb and metabolize MACR, the plants were exposed to 0, 112, 560, or 2,240 μL L^{-1} MACR in an enclosed glass jar (187 mL) for 2 h, and the MACR left in the headspace was quantified (Fig. 5A). The tomato plants absorbed almost all MACR in the headspace at a concentration of 112 μL L^{-1}. At this concentration, almost all MACR absorbed by the tomato was converted into GSH adducts (Fig. 5C). The total GSH level (GSH plus the oxidized form of GSH) was significantly lowered after 2-h exposure to MACR at 112 μL L^{-1} (Fig. 5D). Isobutyraldehyde formation was not detected in this treatment (Fig. 5B). With 560 μL L^{-1} MACR in the vapor phase, approximately 12% of the MACR (corresponding to 69.4 μL L^{-1}) was left in the headspace. At this concentration, the amounts of GSH adducts barely increased from the values found with 112 μL L^{-1} MACR treatment, whereas the total GSH level was lowered to approximately 10% of that found in control leaves. Isobutyraldehyde was emitted from the plants, but accounted for only 7% of the MACR used for the exposure. The amounts of GSH adducts were still almost the same even when the plants were exposed to 2,240 μL L^{-1}. The amount of isobutyraldehyde accounted for 6.5%. Because of the limits of MACR metabolism, a large amount (approximately 54.3%) of the MACR used for exposure remained after 2 h.

Reactive carbonyl species are deleterious to plants at high concentrations (Mano, 2012; Matsui et al., 2012; Farmer and Mueller, 2013). This is because the capacity of plants to detoxify reactive carbonyl species is limited, and surplus chemicals react with biological molecules inside plant tissues. The deleterious effect of MACR that was not detoxified (leftover) in tomato tissue was estimated by measuring the photochemical efficiency (F_v/F_m) ratio as an indicator of stress on photosynthetic machinery (Baker and Rosenqvist, 2004), after exposing tomato plants to different concentrations of MACR vapor for 2 h. The F_v/F_m values were not affected when tomato plants were exposed to MACR vapor at

Table I. *Accumulation of MACR-GSH and MAA-GSH in tomato plants exposed to airflow containing MACR at 20 μL L^{-1}*

Five potted tomato plants were exposed to airflow (at 1.5 L min^{-1}) containing 0 or 20 μL L^{-1} MACR for 6 h in a transparent, fluorinated ethylene-propylene copolymer bag (20–40 L). Then, the amounts of MACR-GSH and MAA-GSH accumulated in tomato leaves were quantified with LC-MS/MS. Mean ± SE (n = 5) is shown. Asterisks indicate a statistically significant difference (t test; **, $P < 0.01$).

Concentration of MACR (nL L^{-1})	0	20
	nmol g^{-1} FW	
MACR-GSH	0.141 ± 0.04	1.47 ± 0.14**
MAA-GSH	2.13 ± 0.43	37.9 ± 2.84**

Table II. *Accumulation of MACR-GSH and MAA-GSH in tomato plants exposed to airflow containing MACR at 100 μL L^{-1}*

Five potted tomato plants were exposed to airflow (at 1.5 L min^{-1}) containing 0 or 100 μL L^{-1} MACR for 6 h in a transparent, fluorinated ethylene-propylene copolymer bag (20–40 L). Then, the amounts of MACR-GSH and MAA-GSH accumulated in tomato leaves were quantified with LC-MS/MS. Mean ± SE (n = 5) is shown. Asterisks indicate a statistically significant difference (t test; **, $P < 0.01$).

Concentration of MACR (nL L^{-1})	0	100
	nmol g^{-1} FW	
MACR-GSH	0.147 ± 0.04	6.51 ± 0.87**
MAA-GSH	0.882 ± 0.16	152.5 ± 15.7**

112 μL L^{-1}, but the value was lowered when the plants were exposed to higher concentrations, such as 560 and 2,240 μL L^{-1} (Fig. 5E). The degree of damage caused by MACR correlated with the amount of MACR left in the jar after 2 h. After the plants were exposed to MACR for 2 h, they were taken out of the jar and incubated for an additional 19 h under the same light and temperature conditions but without MACR. The pretreatment with MACR at 2,240 μL L^{-1} for 2 h resulted in withering of leaves after 19 h, whereas the F_v/F_m values with plants pretreated with 560 μL L^{-1} after 19-h recovery were not different from those pretreated without or with low (112 μL L^{-1}) concentration of MACR vapor (Supplemental Fig. S6).

DISCUSSION

We showed that tomato shoots efficiently absorb MACR in the vapor phase under the experimental conditions used here. The vapor pressure of MACR is 155 mm Hg at 25°C (PubChem, http://www.ncbi.nlm.nih.gov/pccompound); thus, 4.7 μmol of MACR in a 187-mL jar should be mostly in the vapor phase. Henry's law coefficient for MACR is 6.5 ± 0.7 mol L^{-1} atm^{-1} (Iraci et al., 1999). Under equilibrium conditions obeying the ideal gas law, $R_{aq/g} = HLRT$, where $R_{aq/g}$ is the ratio of the compound in aqueous phase to gas phase, H is Henry's law coefficient (mol L^{-1} atm^{-1}), L is the liquid content (cm^3 cm^{-3}; approximately 0.8-cm^3 water content [approximately 80% water content in approximately 1.0 g FW of tomato placed in the jar] in a 187-cm^3 jar [corresponding to 4.28×10^{-3}]), R is the ideal gas constant (0.08206 L atm K^{-1} mol^{-1}), and T is the absolute temperature (298 K; Iraci et al., 1999). Under our experimental conditions, $R_{aq/g}$ was calculated as 0.68; thus, the amount of MACR in the water phase (in tomato tissues) was estimated to be 1.89 μmol while 2.81 μmol of MACR still remained in the vapor phase under equilibrium. The results in this study clearly showed that MACR in the gas phase almost completely disappeared in the presence of tomato shoots. This indicates that MACR is metabolized inside the plant. Metabolite analyses showed that reduction of the double bond conjugated to the carbonyl, reduction of the aldehyde moiety, and glutathionylation played major roles in the metabolism of MACR to support its active uptake (Fig. 6).

Reduction of the double bond conjugated to a carbonyl moiety is one of the pathways for detoxifying cytotoxic reactive carbonyl species harboring an α,β-unsaturated carbonyl moiety (Mano, 2012). In cucumber (*Cucumis sativus*) and Arabidopsis, NADPH-dependent AORs are involved in the reduction of the double bond (Yamauchi et al., 2011). Another pathway for detoxification of reactive carbonyl species reduces the carbonyl to alcohol and is catalyzed by AKRs that also prefer NADPH as the reducing cofactor (Yamauchi et al., 2011; Matsui et al., 2012). The analysis of metabolites in tomato exposed to MACR vapor indicated that both AORs and AKRs were involved in metabolizing MACR in tomato tissues. Because AORs require an α,β-unsaturated carbonyl moiety, isobutyl alcohol should be formed through AOR-dependent reduction of the double bond of MACR to yield isobutyraldehyde, followed by AKR-dependent reduction of isobutyraldehyde to yield isobutyl alcohol. A portion of this isobutyraldehyde was released from the tissue, and a substantial amount of isobutyraldehyde was detected in the jar after 2 h. However, the isobutyraldehyde in the jar almost completely disappeared thereafter, which implies that the tomato plant reabsorbed isobutyraldehyde, dependent on a metabolism to further reduce it to isobutyl alcohol. This observation does not exclude the possibility that a portion of these metabolites is derived from endogenous sources. We found that tomato emitted MACR at a rate of 0.38 ± 0.09 nL g^{-1} FW h^{-1}. Therefore, low but substantial contribution (up to 0.1%) of MACR produced by plants should also be considered.

Because the reducing equivalents (i.e. NADH and NADPH) are essential to both reductases, and their contents in plant tissues are generally less than 10 nmol g^{-1} FW (Queval and Noctor, 2007), regeneration of these cofactors would be necessary to support the reduction to form 40 (MAA in headspace) to 360 (MAA in tomato tissue) nmol g^{-1} FW of the reduced products (Fig. 2). This could be achieved only through continuous regeneration of NADPH and NADH from $NADP^+$ and NAD^+ via the active primary metabolism in intact cells. This indicates that the reduction is accomplished inside the cells, and that it is an active process requiring substantial resources that could otherwise be used for plant growth.

The genes for AOR and AKR form a family, and each member shows distinct substrate specificity (Yamauchi et al., 2011; Saito et al., 2013). As far as we know, an enzyme with high specificity for MACR has not been reported so far; therefore, we do not know if there is a reductase specific to MACR. Identification of the reductase(s) involved in the reduction of MACR to MAA and isobutyl alcohol should be carried out. Because we observed reduction to MAA in tomato tissue even within several seconds after the onset of exposure (Fig. 2B), there should be substantial activity in tomato shoots even before MACR exposure.

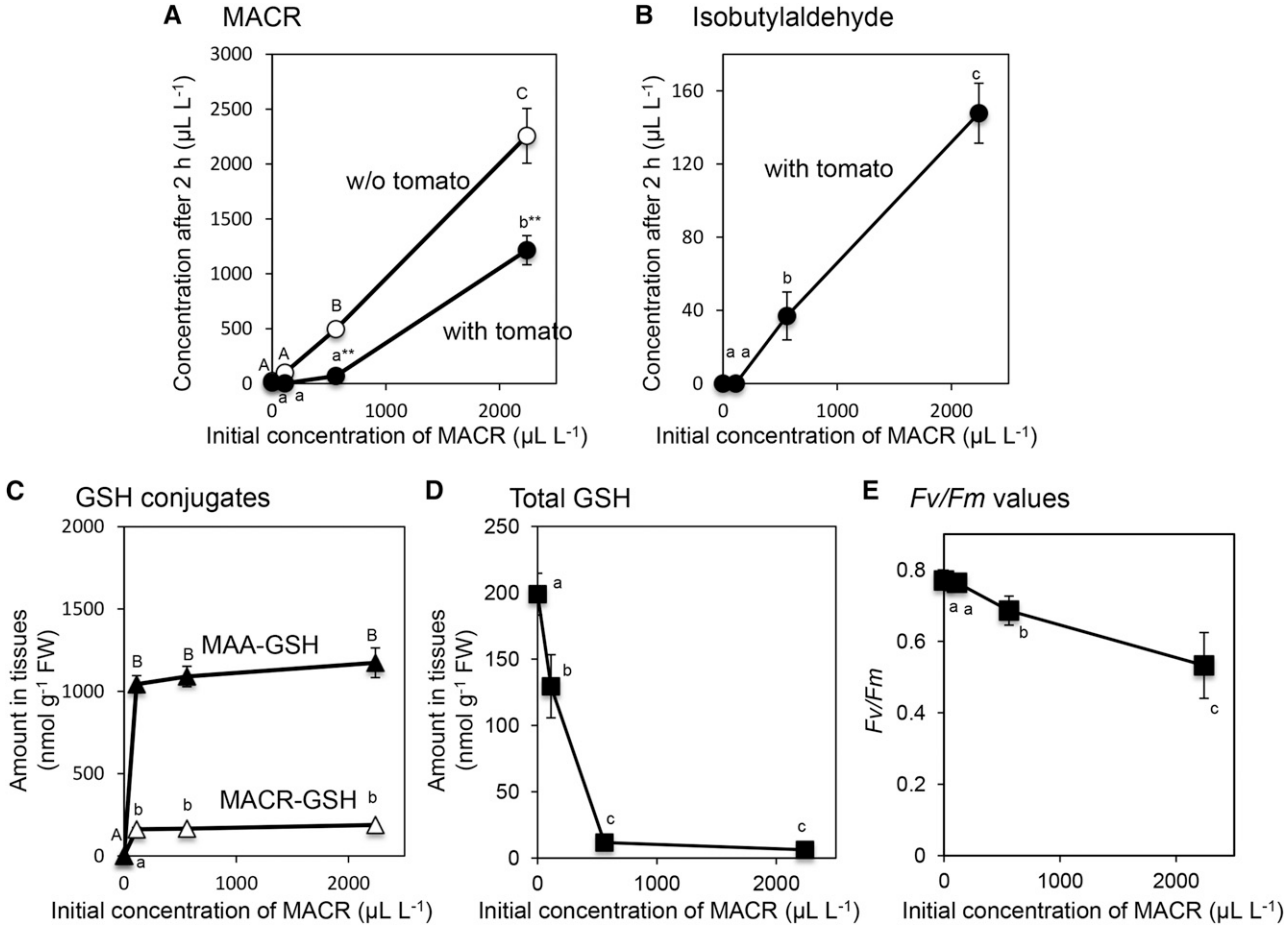

Figure 5. Effect of MACR exposure at 0, 112, 540, or 2,240 μL L^{-1} in a glass jar (187 mL) for 2 h on tomato plants. A, The concentration of MACR left in the headspace of the jar after 2 h in the absence (white circle) and in the presence (black circle) of a tomato plant. B, The concentration of isobutyraldehyde formed and emitted from the plant to the headspace. Isobutyraldehyde was not detected in the absence of tomato. C, The amount of MACR-GSH (white triangles) and MAA-GSH (black triangles) accumulated in tomato leaves. D, Amount of total GSH in tomato leaves. E, F_v/F_m values after treatment. For F_v/F_m measurement, plants in pots were exposed to the given concentration of MACR vapor in a 3-L glass container. Bars represent the mean ± SE; $n = 4$. Different letters indicate a significant difference among MACR concentrations (statistical analysis: A, two-way ANOVA followed by Tukey, $P < 0.05$; B–E, one-way ANOVA followed by Tukey, $P < 0.05$), and asterisks in A indicate significant differences between treatments (**, $P < 0.01$).

Based on the amounts of metabolites formed from MACR, conjugation of MACR with GSH was assumed to be an important mechanism accounting for the uptake of MACR by tomato plants. MACR-GSH was formed spontaneously at pH 6.5 just by mixing MACR and GSH, and we could not detect GST activity in tomato leaves enhancing this spontaneous formation. Therefore, we assume that spontaneous conjugation between MACR and GSH largely accounts for the formation of MACR-GSH in tomato leaves exposed to MACR vapor, and enzymatic formation via GST has little, if any, contribution. The second-order rate constant of MACR and GSH in phosphate buffer (pH 6.8) is as high as 203 L mol^{-1} min^{-1} (Böhme et al., 2010). This high reaction rate explains the quick formation of MACR-GSH adduct well, even without GST.

The amount of GSH in the tomato seedlings used in this study was estimated to be 0.2 μmol g^{-1} FW (compare with Fig. 5D). When a tomato shoot (approximately 1 g FW) was exposed to 112 μL L^{-1} MACR in a 187-mL jar (0.94 μmol of MACR), more than 1 μmol g^{-1} FW of GSH adducts (the sum of MACR-GSH and MAA-GSH) was formed (Fig. 5C). Therefore, de novo replenishment of GSH would be essential for the formation of this amount of GSH adducts. Transgenic tomatoes having lower γ-glutamyl-Cys synthetase and/or glutathione synthetase activities showed lower capacity to decompose chlorothalonil, a fungicide (Yu et al., 2013). The genes for γ-glutamyl-Cys synthetase and GSH synthetase were induced when Arabidopsis was exposed to ozone (Yoshida et al., 2009). Taken together, a system to replenish GSH is one of the keys to meeting the demand brought about under stressed conditions.

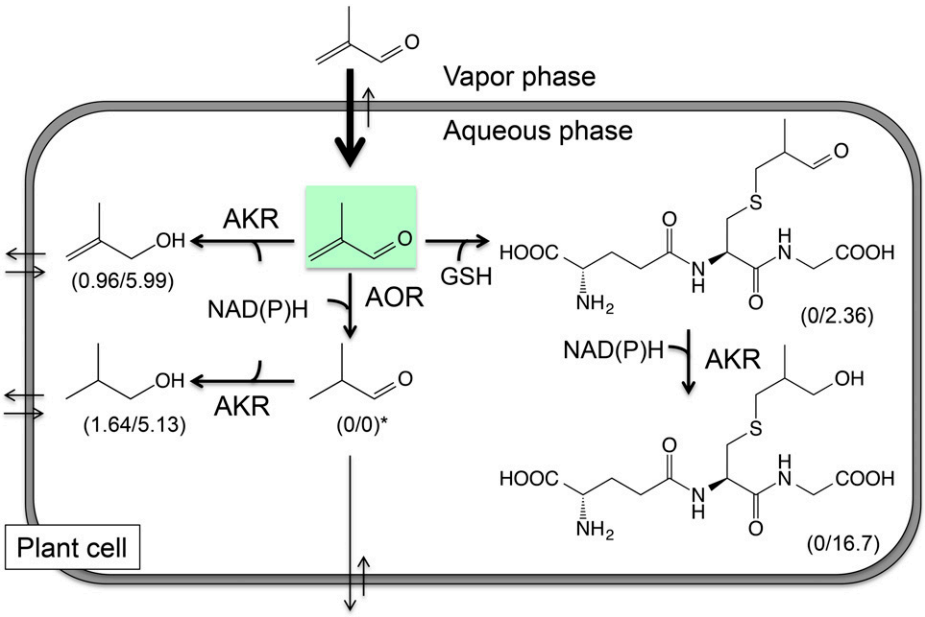

Figure 6. Metabolism inside cells supports the absorption of MACR from the vapor phase. MACR in the vapor phase is distributed into the cell interior at a given equilibrium defined by Henry's law. Because MACR distributed in cells is quickly metabolized into its reduced form and its GSH adducts, the concentration of MACR in the cells is lowered. Accordingly, more MACR is partitioned into the cell. Conversion rates of MACR exposed at 560 μL L^{-1} for 2 h are shown in parentheses (percentage, outside/inside). AOR, Alkenal/one oxidoreductase; AKR, aldo-keto reductase.

MACR-GSH was further reduced to form MAA-GSH by a reductase in an NADPH-dependent manner. The MACR-GSH to MAA-GSH reduction activity was induced after exposing plants to MACR, which implies that the enzyme responsible for this reduction is involved in plant responses to the stress caused by MACR exposure. In tobacco, GSH adducts with keto fatty acids and 12-oxophytodienoic acid were found with the ketone group; conversely, in tobacco and grapevine, a GSH adduct formed from (*E*)-2-hexenal was found as its reduced form [i.e. *S*-3-(hexan-1-ol)-glutathione; Davoine et al., 2005, 2006; Kobayashi et al., 2011]. Thus, it was suggested that the reductase acting on GSH adducts preferred aldehydes to ketones. MAA-GSH persisted for at least 6 h, but its amount was slightly decreased at 24 h. Degradation of the GSH adduct catalyzed by γ-glutamyl transferase, such as that found in grapevine (Kobayashi et al., 2011), might be involved in the degradation of MAA-GSH.

At a lower concentration of MACR (112 μL L^{-1} in a 187-mL jar), almost all of the MACR was absorbed by the tomato plant and metabolized essentially into its GSH adducts (Fig. 5). Therefore, the tomato suffered few deleterious effects on its photosynthetic apparatus at this low concentration of MACR, even though the total GSH levels were lowered to 60% of the control. Because of the efficient removal of MACR through glutathionylation at a low concentration, the reduction to form isobutyraldehyde was not occurring. At higher MACR concentrations, such as 560 and 2,240 μL L^{-1}, the amount of GSH adducts formed in the tissue was almost the same as in the plant exposed to 112 μL L^{-1} MACR. This should essentially be because of limited GSH availability in the tomato tissue. The replenishment of GSH probably fell short, and as a result, the GSH pool was almost empty shortly after the plant was exposed to MACR at 560 and 2,240 μL L^{-1}. Reduction of MACR became apparent at high concentrations, which would partly account for its detoxification. However, the ability to reduce MACR was insufficient at high concentrations, and some of the MACR partitioned into tissues would remain as MACR. The substantial concentrations of MACR in the vapor phase after 2-h exposure at 560 and 2,240 μL L^{-1} clearly suggested that a substantial amount of MACR stayed in the tissues, according to Henry's law. At 2 h after exposing tomato shoots to 2,240 μL L^{-1} MACR in a closed jar, 1,331 μL L^{-1} MACR still remained in the vapor phase, and under these conditions, it was assumed that the MACR concentration in the tissue might go up to 7.55 μmol g FW^{-1}. The leftover from MACR metabolism had a deleterious effect on plant cells as evidenced by the suppression of PSII activity with MAC exposure at 560 and 2,240 μL L^{-1}.

These lines of evidence indicated that MACR uptake was largely supported by MACR metabolism inside the tomato tissue, and that spontaneous reaction of MACR with GSH was most responsible for its metabolism, especially when the MACR concentration was less than 112 μL L^{-1}. The reduction of MACR might support its metabolism, especially at higher concentrations. Thus, the amount of GSH in the tissue is one of the keys to the cleansing of oVOCs from the atmosphere by vegetation. Many other reactions of oVOCs, such as oligomer formation (Liu et al., 2012) or reaction with hydrogen peroxide (Schöne and Herrmann, 2014), are still possible. Their contribution to the cleansing of oVOCs by vegetation should also be evaluated in future studies.

There are many chemical species of oVOCs in the atmosphere, and the absorption rates determined for them under realistic conditions using flow systems vary widely. Tani and Hewitt (2009) reported that plants

absorbed aldehydes more efficiently than the corresponding ketones. Acetone, for example, was only partly taken up by plants at the beginning of exposure because of the partition into plant tissues, but was not continuously taken up, probably because no metabolism is expected for this ketone. The situation is also the same with *Populus nigra* and *Camellia sasanqua*. In these species, acrolein and methyl ethyl ketone were taken up efficiently, but acetone, acetonitrile, isobutyl methyl ketone, chloroform, and benzene were essentially not taken up (Omasa et al., 2000). These observations also support that metabolism inside plant tissues is indispensable for cleansing oVOCs from the atmosphere. In our experimental system, at a reasonably low MACR concentration with a flow system simulating the natural environment, glutathionylation proceeded quite efficiently, and as much as 30% to 40% of the MACR flowing over tomato plants was absorbed and converted into its adducts. This implies that glutathionylation is one of the major metabolic pathways supporting the active absorption of oVOCs by tomato plants.

Harnessing the high ability of plants to metabolize oVOCs would be one way to manage air pollutants. To cope with the accumulation of anthropogenic as well as biogenic oVOCs, first we need to know the metabolic pathways responsible for their uptake by vegetation. We should investigate whether glutathionylation and reduction reactions are intrinsic to the cleansing of oVOCs in other plant species. Also, continuous monitoring of GSH adducts formed from some oVOCs in the field would give insight into the contribution of glutathionylation to the deposition of oVOCs to vegetation.

MATERIALS AND METHODS

Plant Materials and Growth Conditions

Seeds of wild-type tomato (*Solanum lycopersicum* 'Microtom') plants obtained from the Agriculture and Forestry Research Center were grown under 14-h-light (fluorescent lights at 60 μmol m^{-2} s^{-1})/10-h-dark conditions at 25°C on soil composed of vermiculite and Takii Tanemakibaido (Takii and Co. Ltd.; volume ratio of 1:1) in a plastic pot (6-cm i.d.). The tomato plants were watered every 3 d with Hyponex Concentrated Liquid (HYPONeX JAPAN Co. Ltd.) diluted to 0.1% (v/v).

MACR Vapor Treatment on Tomato Plants

The aerial parts of 3- to 4-week-old tomato were cut at the stem-root junction. The cut surface was covered with water-soaked cotton and then aluminum foil. The shoot was exposed to MACR (Sigma-Aldrich) vapor in a 187-mL glass jar. For the treatment, 9.35 μL of MACR dissolved in 3.5% (w/v) Tween 20 at 0.5 M was impregnated in a cotton swab, and the swab was attached to the aluminum cap of the jar. The concentration of MACR in the inner space of the jar would be 560 μL L^{-1}. For treatment at lower concentrations, the MACR solution was sequentially diluted with 3.5% (w/v) Tween 20 (e.g. 0.1 M for 112 μL L^{-1} or 0.02 M for 22.4 μL L^{-1}), and 9.35 μL was impregnated in the cotton swab. For 2,240 μL L^{-1}, 131 μg of neat MACR was directly impregnated in the cotton swab. The jar was placed in a chamber under the same conditions used to grow the tomato plants. Control plants were exposed to water vapor. A jar without a plant was also prepared as a control to see the spontaneous degradation of MACR under the experimental conditions used here. To measure the F_v/F_m values of the tomato, we used intact tomato plants without cutting the aerial part from pots to follow recovery from damage caused by MAC exposure at 19 h after the treatment. Three tomato plants grown in soil in pots were exposed to MACR vapor in a 3-L glass jar and incubated under the same conditions as described above.

To expose tomato plants to airflow containing vaporized MACR, we enclosed five tomato plants grown in pots with soil in a transparent, fluorinated ethylene-propylene copolymer bag (20–40 L). The open side of the bag was closed with a cable tie, and air was introduced into the bag via an inlet port at a flow rate of 1.5 L min^{-1}. VOCs and other contaminants including ozone from the inflow air were removed with a platinum catalysis heated to 400°C. The plants were illuminated with a 400-W metal halide lamp (D400, Toshiba LiTec). The photosynthetic photon flux density was held at 100 μmol m^{-2} s^{-1} at the top of the plants. The temperature in the bag was measured with T-type fine-wire thermocouples and set at 25°C to 27°C during the exposure (for 6 h). Water vapor concentrations and the carbon dioxide concentrations of the inlet and outlet air were measured with a CO_2/H_2O gas analyzer (LI-840A, LI-COR). A constant concentration of MACR vapor was maintained with a gas generator (PD-1B, Gastec) and adjusted to 20 or 100 nL L^{-1} by mixing the MAC-containing air with clean air generated by blowing room air through a platinum catalyst heated to 400°C at a given ratio. After exposure, the leaves were harvested and snap frozen with liquid nitrogen for further analysis. To quantify the amounts of isoprene and MACR emitted from tomatoes, tomato plants in pots were placed in the airflow system bag as above, and a portion of the outlet air was introduced through an adsorbent tube containing 200 mg of Tenax-TA and 100 mg of Carbotrap (Sigma-Aldrich) at a flow rate of 200 mL min^{-1} for 20 min using a portable pump (MP-Sigma30, Shibata Inc.). The collected samples were identified and quantified with a GC mass spectrometer (QP5050A, Shimadzu) equipped with a thermal desorption system (TurboMatrix ATD, Perkin Elmer Instruments). Compound separation was achieved using an SPB-5 capillary column (50 m × 25 mm, 1-mm film thickness, Sigma-Aldrich; Mochizuki et al., 2014).

Measurement of the F_v/F_m Ratio

The F_v/F_m ratio, as a parameter relating to the maximum quantum yield of PSII, was estimated from chlorophyll fluorescence measurements using a pulse amplitude-modulated fluorometer (Mini-PAM photosynthesis yield analyzer, Walz). The saturation pulse duration was 0.8 s with an intensity level of approximately 8,300 μmol m^{-2} s^{-1}. After exposure to MACR vapor, the tomato plants were placed in the dark for 30 min, and then fluorescence measurements were conducted at the center of the leaves.

Measurement of MACR in the Headspace of the Glass Jar

A tomato plant was exposed to 560 μL L^{-1} (in vapor) MACR in a glass jar. After closing the cap, the headspace air (10 mL) in the jar was collected with a gas-tight syringe through a silicon rubber septum (6-mm i.d.) inserted into a hole made at the center of the lid. The air was introduced into a closed glass vial containing a mixture of acetonitrile (400 μL), 20 mM 2,4-dinitrophenylhydrazine (100 μL), formic acid (20 μL), and 10 mM 2-ethylhexanal (internal standard [IS], 10 μL; Alfa Aesar). The mixture was vigorously vortexed for 2 min and left for 30 min under dark conditions at room temperature. After incubation, the mixture was transferred to a glass tube containing 1 mL of water and 2 mL of ethyl acetate, mixed vigorously, and centrifuged at 1,000*g* for 10 min. The organic layer was collected and subjected to HPLC analysis. The hydrazone derivatives were analyzed using an HPLC system with a Mightysil RP-18 GP column (Kanto Chemical Co.) as described by Matsui et al. (2009). For the quantification of each compound, calibration curves were constructed using IS and standard compounds, MACR, and isobutyraldehyde (Wako Pure Chemical Industries, Ltd.).

Analysis of the Metabolites Derived from MACR in the Headspace and Tomato Tissues

The air (10 mL) in the jar, obtained with a gas-tight syringe, was introduced into a tightly closed glass vial containing 1 mL of CH_2Cl_2 with 50 ng mL^{-1} nonyl acetate (Tokyo Chemical Industry Co.) as an IS. The vial was vigorously vortexed for 2 min, and the solution was subsequently concentrated with N_2 gas to approximately 100 μL for GC-MS analysis using a GC mass spectrometer (QP-5050, Shimadzu) equipped with a DB-Wax column (30-m length × 0.25-mm i.d. × 0.25-μm film thickness, Agilent Technologies). The column temperature was programmed as follows: 40°C for 5 min, increasing by 10°C min^{-1} to 200°C for 5 min. The carrier gas (helium) was delivered at 86.1 kPa. The sample size

was 1 μL, and the split ratio was 2. The temperatures of the injector and interface were 240°C and 200°C, respectively. The mass detector was operated in the electron impact mode with ionization energy of 70 eV. Identification of the alcohols was performed by comparing their retention times and mass spectra with those of standard compounds, MAA (Tokyo Chemical Industry Co.), and isobutyl alcohol (Sigma-Aldrich Co.). The amount of each compound was calculated with a calibration curve based on the area ratio of the sample to the IS.

To analyze the metabolites derived from MACR in tomato leaves, the leaves were wrapped in aluminum foil and snap frozen in liquid nitrogen. The frozen leaves wrapped in foil were crushed with a hammer to make leaf powder in liquid nitrogen. The powder was placed in a plastic tube with eight stainless beads (3 mm in diameter) at −80°C until extraction. The stored samples were further crushed with a beads cell disruptor (Micro Smash MS100R, TOMY Digital Biology, Co.) for 1 min at 3,500 rpm, keeping the materials frozen. One milliliter of CH_2Cl_2 containing 500 ng mL^{-1} nonyl acetate as an IS was added to the tomato leaf powder (100 mg) and homogenized for 1 min at 3,500 rpm with the beads cell disruptor. The sample was centrifuged for 10 min at 12,000*g* with the T16A31 rotor (Hitachi Koki, Co.). The CH_2Cl_2 layer was transferred into a new glass tube. After concentration with N_2 gas to 100 μL, the compounds in the solution were analyzed by GC-MS as described above. The amounts of alcohols were calculated with the corresponding calibration curves constructed with authentic compounds based on the area ratio to the IS.

Synthesis of GSH Conjugates

To obtain MACR-GSH with high purity, 3.25 mmol of GSH (Wako Pure Chemical Industries, Ltd.) was mixed with an excess amount (24.2 mmol) of MACR in 20 mM borate buffer, pH 10.0, and reacted for 1 h under an argon atmosphere. The reaction was stopped by adjusting the pH to 4.0 with 10% (v/v) formic acid, and the surplus MACR was evaporated out with N_2 gas flow. Complete consumption of GSH was confirmed by thin-layer chromatography analysis on silica plates (Silica gel 60 F254, Merck KGaA) using acetonitrile/water/acetic acid (80/20/0.1, v/v) as the developing solvent. The compounds were visualized with anisaldehyde or ninhydrin reagent. The product was freeze dried and subjected to LC-MS/MS analysis. A total ion chromatogram obtained with the enhanced mass (EMS) mode indicated greater than 90% purity of MACR-GSH. MAA-GSH was synthesized by adding an excess amount of $NaBH_4$ to MACR-GSH in 20 mM borate buffer, pH 10.0. Identification of the compounds was performed by LC-MS/MS with EMS mode (Supplemental Fig. S4) using a 3200 Q-TRAP LC/MS/MS System (AB Sciex) equipped with a Prominence UFLC (Shimadzu). The products were separated on a Mightysil RP-18 column (150- × 2-mm i.d.) with a binary gradient consisting of water: formic acid (100:0.1, v/v, solvent A) and acetonitrile:formic acid (100:0.1, v/v, solvent B). The run consisted of 100% A for 5 min, a linear increase from 100% A to 100% B over 25 min (flow rate of 0.2 mL min^{-1}), and 100% B for 2 min. Compounds were detected by MS/MS using electrospray ionization in the positive ion mode (ion spray voltage, 5,000 V, nitrogen as both the curtain gas [set to 20 arbitrary units] and collision gas [set to high]; collision energy, 19 V; scan range, *m/z* 100–1,200; scan speed, 4,000 D s^{-1}; declustering potential, 26 V).

Analysis of GSH Adducts in Tomato Leaves

The frozen powder prepared from tomato leaves (80 mg) was suspended in 1 mL of 20 mM borate buffer, pH 4.0, containing 5 μg of *S*-hexylglutathione (Sigma-Aldrich Co.) as an IS. The GSH adducts were extracted with a beads cell disruptor for 1 min at 3,500 rpm. The suspension was centrifuged at 8,000*g* for 15 min at 4°C. The supernatant was filtered through an Ekicrodisc 3 (HPLC certified, 0.45 μm, 3 mm; Pall Corporation). GSH conjugates in the extract were scanned by analysis in the EMS mode as shown above or in the neutral loss mode, which permitted the determination of the *m/z* ratio of pseudomolecular ions undergoing neutral loss of 75 mass units (part of Gly) upon fragmentation of the compounds under the same MS conditions used in EMS mode. The compounds were identified by comparing the mass spectra (obtained with EMS mode) and their retention times with those of standard compounds. For quantification of GSH conjugates in the sample, LC-MS/MS analysis in the multiple reaction monitoring (MRM) mode was performed. A calibration curve was constructed with the synthesized MACR-GSH and MAA-GSH based on their area ratio to *S*-hexylglutathione. The parameters used for MRM detection are shown in Supplemental Table S1. Total GSH (GSH + oxidized form of GSH) was determined with the enzymatic recycling assay based on GSH reductase and 5,5′-dithiobis-(2-nitrobenzoic acid) as described by Griffith (1980).

GST and Reductase Assay

The crude enzyme solution for GST and reductase assay was prepared according to a procedure described previously (Davoine et al., 2006). Tomato leaves (0.5–0.7 g FW) were homogenized with 50 mM potassium phosphate buffer (pH 7.2) containing 2 mM dithiothreitol, 0.01% (w/v) Triton X-100, 1 mM EDTA, and 8% (w/v) polyclar VT (Wako Pure Chemical Industries, Ltd.) using a mortar and pestle. After filtration with cheesecloth, the sample was centrifuged at 14,500*g* at 4°C for 20 min. The supernatant was used for the assay. The protein content was determined using a Bio-Rad Protein Assay.

For the GST activity assay, the absorption at 340 nm was monitored with a reaction solution (1 mL) containing 1 mM 1-chloro-2,4-dinitrobenzene, 1.5 mM GSH, and crude enzyme solution (100 μL) in 50 mM potassium phosphate buffer, pH 7.2, at 25°C for 3 min. To estimate the GST activity to form MACR-GSH, a reaction solution (0.5 mL) containing 0.2 mM MACR, 0.3 mM GSH, and crude enzyme solution (10 μL) in 100 mM potassium phosphate buffer, pH 7.2, was prepared and reacted for 1 and 10 min. The reaction was stopped by adjusting the pH to 4.0 using 10% (v/v) formic acid. The mixture was filtered and subjected to LC-MS/MS analysis to quantify the MACR-GSH. Control reactions were done without enzyme solution and with heat-denatured (100°C for 10 min) enzyme solution.

The enzymatic activity to reduce MACR-GSH to MAA-GSH was examined by monitoring the product with LC-MS/MS. A reaction mixture (500 μL) containing 0.2 mM MACR-GSH, 4 mM NADH or NADPH, and crude enzyme solution (10 μL) in 50 mM potassium phosphate buffer, pH 7.2, was reacted for 10 min. After incubation, the reaction was stopped by adjusting the pH to 4.0. The GSH adducts formed through enzymatic reaction were quantified by LC-MS/MS analysis in MRM mode.

Statistics

Statistical analyses were conducted using Excel toukei (Social Survey Research Information Co.). When two factors were considered, we used two-way ANOVA followed by Tukey's post-hoc test, whereas for single factors, one-way ANOVA followed by Tukey's post-hoc test was applied. The accumulation of GSH adduct in the airflow experiment was evaluated with a *t* test.

Supplemental Data

The following supplemental materials are available.

Supplemental Figure S1. Total ion chromatogram with GC-MS of reduced metabolites from MACR in the headspace and in tomato tissues.

Supplemental Figure S2. A representative chromatogram of a mixture of synthetic MACR-GSH, MAA-GSH, and Hex-GSH (included as internal standard) obtained with the MRM mode of LC-MS/MS.

Supplemental Figure S3. MS profile of synthesized MACR-GSH and MAA-GSH and the corresponding peaks detected in tomato tissues.

Supplemental Figure S4. Chromatogram obtained with the neutral loss mode (−75 D) of LC-MS/MS to examine GSH conjugates formed in tomato leaves after exposure to MACR.

Supplemental Figure S5. Effect of addition of crude enzyme solution prepared from tomato leaves on the reaction between GSH and MACR.

Supplemental Figure S6. Consequence of MACR exposure at 0, 112, 540, or 2240 μL L^{-1} for 2 h on tomato plants.

Supplemental Table S1. Parameters used for MRM analysis of GSH conjugates.

Received July 10, 2015; accepted July 12, 2015; published July 13, 2015.

LITERATURE CITED

Atkinson R, Arey J (2003) Atmospheric degradation of volatile organic compounds. Chem Rev **103:** 4605–4638

Baker NR, Rosenqvist E (2004) Applications of chlorophyll fluorescence can improve crop production strategies: an examination of future possibilities. J Exp Bot **55:** 1607–1621

Böhme A, Thaens D, Schramm F, Paschke A, Schüürmann G (2010) Thiol reactivity and its impact on the ciliate toxicity of α,β-unsaturated aldehydes, ketones, and esters. Chem Res Toxicol **23:** 1905–1912

Davoine C, Douki T, Iacazio G, Montillet JL, Triantaphylidès C (2005) Conjugation of keto fatty acids to glutathione in plant tissues. Characterization and quantification by HPLC-tandem mass spectrometry. Anal Chem **77:** 7366–7372

Davoine C, Falletti O, Douki T, Iacazio G, Ennar N, Montillet JL, Triantaphylidès C (2006) Adducts of oxylipin electrophiles to glutathione reflect a 13 specificity of the downstream lipoxygenase pathway in the tobacco hypersensitive response. Plant Physiol **140:** 1484–1493

Farmer EE, Mueller MJ (2013) ROS-mediated lipid peroxidation and RES-activated signaling. Annu Rev Plant Biol **64:** 429–450

Fedrizzi B, Guella G, Perenzoni D, Gasperotti M, Masuero D, Vrhovsek U, Mattivi F (2012) Identification of intermediates involved in the biosynthetic pathway of 3-mercaptohexan-1-ol conjugates in yellow passion fruit (*Passiflora edulis* f. *flavicarpa*). Phytochemistry **77:** 287–293

Goldstein AH, Galbally IE (2007) Known and unknown organic constituents in the Earth' s atmosphere. Environ Sci Technol **41:** 1514–1521

Griffith OW (1980) Determination of glutathione and glutathione disulfide using glutathione reductase and 2-vinylpyridine. Anal Biochem **106:** 207–212

Guenther A, Hewitt CN, Erickson D, Fall R, Geron C, Graedel T, Harley P, Klinger L, Lerdau M, McKay WA, et al (1995) A global model of natural volatile organic compound emissions. J Geophys Res **100:** 8873–8892

Iraci LT, Baker BM, Tyndall GS, Orlando JJ (1999) Measurements of the Henry's law coefficients of 2-methyl-3-buten-2-ol, methacrolein, and methylvinyl ketone. J Atmos Chem **33:** 321–330

Jardine KJ, Meyers K, Abrell L, Alves EG, Yanez Serrano AM, Kesselmeier J, Karl T, Guenther A, Chambers JQ, Vickers C (2013) Emissions of putative isoprene oxidation products from mango branches under abiotic stress. J Exp Bot **64:** 3697–3708

Jardine KK, Monson RK, Abrell L, Saleska SR, Arneth A, Jardine A, Ishida FI, Serrano AMY, Arataxo P, Karl T, et al (2012) Within-plant isoprene oxidation confirmed by direct emissions of oxidation products methyl vinyl ketone and methacrolein. Glob Change Biol **18:** 973–984

Kalogridis C, Gros V, Sarda-Esteve R, Langford B, Loubet B, Bonsang B, Bonnaire N, Nemitz E, Genard AC, Boissard C, et al (2014) Concentrations and fluxes of isoprene and oxygenated VOCs at a French Mediterranean oak forest. Atmos Chem Phys **14:** 10085–10102

Karl T, Harley P, Emmons L, Thornton B, Guenther A, Basu C, Turnipseed A, Jardine K (2010) Efficient atmospheric cleansing of oxidized organic trace gases by vegetation. Science **330:** 816–819

Kirch HH, Bartels D, Wei Y, Schnable PS, Wood AJ (2004) The ALDH gene superfamily of Arabidopsis. Trends Plant Sci **9:** 371–377

Kobayashi H, Takase H, Suzuki Y, Tanzawa F, Takata R, Fujita K, Kohno M, Mochizuki M, Suzuki S, Konno T (2011) Environmental stress enhances biosynthesis of flavor precursors, *S*-3-(hexan-1-ol)-glutathione and *S*-3-(hexan-1-ol)-L-cysteine, in grapevine through glutathione *S*-transferase activation. J Exp Bot **62:** 1325–1336

Liu Y, Siekmann F, Renard P, El Zein A, Salque G, El Haddad I, Temime-Roussel B, Voisin D, Thissen R, Monod A (2012) Oligomer and SOA formation through aqueous phase photooxidation of methacrolein and methyl vinyl ketone. Atmos Environ **49:** 123–129

Liu YJ, Herdlinger-Blatt I, McKinney KA, Martin ST (2013) Production of methyl vinyl ketone and methacrolein via the hydroperoxyl pathway of isoprene oxidation. Atmos Chem Phys **13:** 5715–5730

Mano J (2012) Reactive carbonyl species: their production from lipid peroxides, action in environmental stress, and the detoxification mechanism. Plant Physiol Biochem **59:** 90–97

Matsui K, Sugimoto K, Kakumyan P, Khorobrykh SA, Mano J (2009) Volatile oxylipins and related compounds formed under stress in plants. Methods Mol Biol **580:** 17–28

Matsui K, Sugimoto K, Mano J, Ozawa R, Takabayashi J (2012) Differential metabolisms of green leaf volatiles in injured and intact parts of a wounded leaf meet distinct ecophysiological requirements. PLoS One **7:** e36433

Meldau DG, Meldau S, Hoang LH, Underberg S, Wünsche H, Baldwin IT (2013) Dimethyl disulfide produced by the naturally associated bacterium *bacillus* sp B55 promotes *Nicotiana attenuata* growth by enhancing sulfur nutrition. Plant Cell **25:** 2731–2747

Mochizuki T, Tani A, Takahashi Y, Saigusa N, Ueyama M (2014) Long-term measurement of terpenoid flux above a *Larix kaempferi* forest using a relaxed eddy accumulation method. Atmos Environ **83:** 53–61

Omasa K, Tobe K, Hosomi M, Kobayashi M (2000) Absorption of ozone and seven organic pollutants by *Populus nigra* and *Camellia sasanqua.* Environ Sci Technol **34:** 2498–2500

Otsuka M, Kenmoku H, Ogawa M, Okada K, Mitsuhashi W, Sassa T, Kamiya Y, Toyomasu T, Yamaguchi S (2004) Emission of *ent*-kaurene, a diterpenoid hydrocarbon precursor for gibberellins, into the headspace from plants. Plant Cell Physiol **45:** 1129–1138

Queval G, Noctor G (2007) A plate reader method for the measurement of NAD, NADP, glutathione, and ascorbate in tissue extracts: Application to redox profiling during *Arabidopsis* rosette development. Anal Biochem **363:** 58–69

Saito R, Shimakawa G, Nishi A, Iwamoto T, Sakamoto K, Yamamoto H, Amako K, Makino A, Miyake C (2013) Functional analysis of the AKR4C subfamily of *Arabidopsis thaliana*: model structures, substrate specificity, acrolein toxicity, and responses to light and [CO_2]. Biosci Biotechnol Biochem **77:** 2038–2045

Schöne L, Herrmann H (2014) Kinetic measurements of the reactivity of hydrogen peroxide and ozone towards small atmospherically relevant aldehydes, ketones and organic acids in aqueous solutions. Atmos Chem Phys **14:** 4503–4514

Sugimoto K, Matsui K, Iijima Y, Akakabe Y, Muramoto S, Ozawa R, Uefune M, Sasaki R, Alamgir KM, Akitake S, et al (2014) Intake and transformation to a glycoside of (*Z*)-3-hexenol from infested neighbors reveals a mode of plant odor reception and defense. Proc Natl Acad Sci USA **111:** 7144–7149

Tani A, Hewitt CN (2009) Uptake of aldehydes and ketones at typical indoor concentrations by houseplants. Environ Sci Technol **43:** 8338–8343

Tani A, Tobe S, Shimizu S (2013) Leaf uptake of methyl ethyl ketone and croton aldehyde by *Castanopsis sieboldii* and *Viburnum odoratissimum* saplings. Atmos Environ **70:** 300–306

Yamauchi Y, Hasegawa A, Taninaka A, Mizutani M, Sugimoto Y (2011) NADPH-dependent reductases involved in the detoxification of reactive carbonyls in plants. J Biol Chem **286:** 6999–7009

Yoshida S, Tamaoki M, Ioki M, Ogawa D, Sato Y, Aono M, Kubo A, Saji S, Saji H, Satoh S, et al (2009) Ethylene and salicylic acid control glutathione biosynthesis in ozone-exposed *Arabidopsis thaliana.* Physiol Plant **136:** 284–298

Yu GB, Zhang Y, Ahammed GJ, Xia XJ, Mao WH, Shi K, Zhou YH, Yu JQ (2013) Glutathione biosynthesis and regeneration play an important role in the metabolism of chlorothalonil in tomato. Chemosphere **90:** 2563–2570